Available online at www.sciencedirect.com
SCIENCE DIRECT®
Journal of Sound and Vibration 260 (2003) 927–947
JOURNAL OF SOUND AND VIBRATION
www.elsevier.com/locate/jsvi

Linear and non-linear control techniques applied to actively lubricated journal bearings

R. Nicoletti[1,*], I.F. Santos[2]

[1] *FEM/DPM, Department of Mechanical Design, UNICAMP, State University of Campinas, SP Campinas 13083-970, Brazil*
[2] *MEK, Department of Mechanical Engineering, DTU, Technical University of Denmark, Lyngby, Denmark*

Received 3 October 2001; accepted 2 May 2002

Abstract

The main objectives of actively lubricated bearings are the simultaneous reduction of wear and vibration between rotating and stationary machinery parts. For reducing wear and dissipating vibration energy until certain limits, one can use the conventional hydrodynamic lubrication. For further reduction of shaft vibrations one can use the active lubrication action, which is based on injecting pressurized oil into the bearing gap through orifices machined in the bearing sliding surface. The design and efficiency of some linear (PD, PI and PID) and a non-linear controller, applied to a tilting-pad journal bearing, are analysed and discussed. Important conclusions about the application of integral controllers, responsible for changing the rotor-bearing equilibrium position and consequently the "passive" oil film damping coefficients, are achieved. Numerical results show an effective vibration reduction of unbalance response of a rigid rotor, where the PD and the non-linear P controllers show better performance for the frequency range of study (0–80 Hz). The feasibility of eliminating rotor-bearing instabilities (phenomena of whirl) by using active lubrication is also investigated, illustrating clearly one of its most promising applications.
© 2002 Elsevier Science Ltd. All rights reserved.

1. Introduction

Taking advantage of the oil film load capacity in hydrodynamic bearings as an active device, in order to improve the machine dynamic behaviour, is an idea that has been investigated by many authors during the last two decades (Refs. [1–15]). Initially, the bearings were mounted on linear actuators ([1,2]) and the control action was indirect. In other words, hydraulic or electromagnetic actuators dynamically moved the bearing housing, consequently causing changes in the gap and

*Corresponding author. Tel.: +55-19-3788-3186; fax: +55-19-3289-3722.
E-mail address: rodrigo@fem.unicamp.br (R. Nicoletti).

0022-460X/03/$ - see front matter © 2002 Elsevier Science Ltd. All rights reserved.
PII: S0022-460X(02)00951-3

the hydrodynamic conditions. However, the fact that the control system must support the bearing house, and the rotor itself, requires the actuators to be very robust. This could be a drawback in applying such a system to heavy equipment (hydro-turbines, turbo-generators and compressors). An alternative solution was to locate the actuators inside tilting-pad bearings where, by hydraulic chambers, the position of the shoes could be changed, and thus the machine rotor dynamics altered [4]. This active bearing had the disadvantage of the complexity of its chambers, together with the structural limitations of their components. Hence, active bearings based on injecting pressurized oil directly into the oil film began to be investigated due to its simplicity of concept [5,7,8].

The actively lubricated bearing under investigation is built from four tilting pads, in a load-on-pad configuration, as shown in Fig. 1. The control action over the rotating shaft is made by injecting oil into the bearing gap through machined bores in the pads (Fig. 2). By coupling servo valves to the pads in the vertical and horizontal directions (Fig. 1), the pressure of the injected oil can be controlled. Thus, the hydrodynamic pressure and temperature distribution in the gap (main mechanism of bearing load capacity) may be altered among the different pads [9–11]. Rotating shaft vibration can also be attenuated with help of control techniques as can be seen in Santos and Scalabrin [12]. It is important to emphasise that conventional lubrication is still the main source of load capacity in this hybrid bearing, and the use of radial active lubrication in a special type of journal bearing, the tilting-pad journal bearings (TPJB), has a strong advantage because there remain no cross-coupling effects between orthogonal directions [14].

The aim of this work is to investigate the efficiency of some linear and non-linear control techniques applied to a rotor-bearing system supported by an actively lubricated tilting-pad bearing. The design and efficiency of some linear (PD, PI and PID) and a non-linear controller are analysed and discussed, recalling that integral controllers are able to change the operational position of the rotor inside of the bearing and, consequently, are also able to change the oil film coefficients (damping and stiffness). The control laws of linear PI, PD and PID controllers and of a non-linear P controller are deduced and added to the non-linear equations of motion which describe the system. Numerical simulations are performed in order to obtain the system unbalance

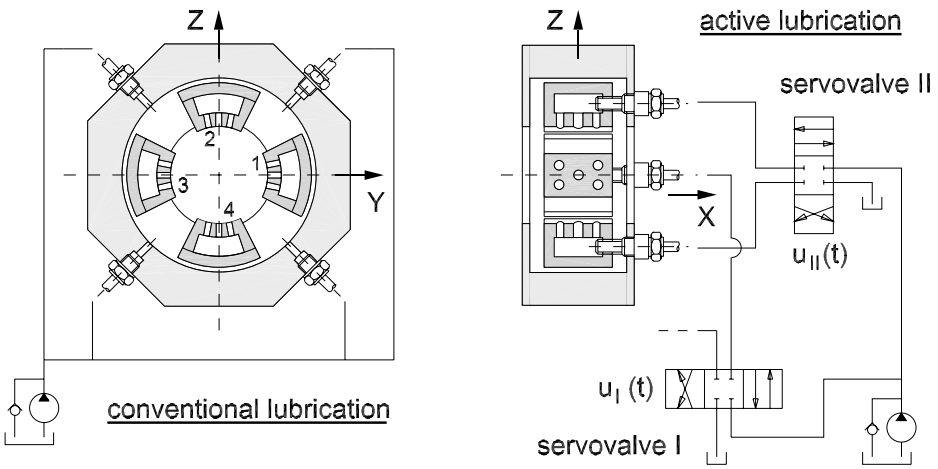

Fig. 1. Active tilting-pad bearing with injection system.

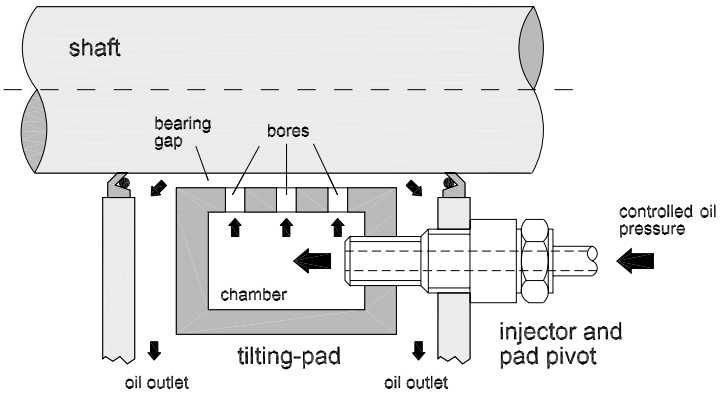

Fig. 2. Schematic view of the oil injection system of the active tilting-pad bearing.

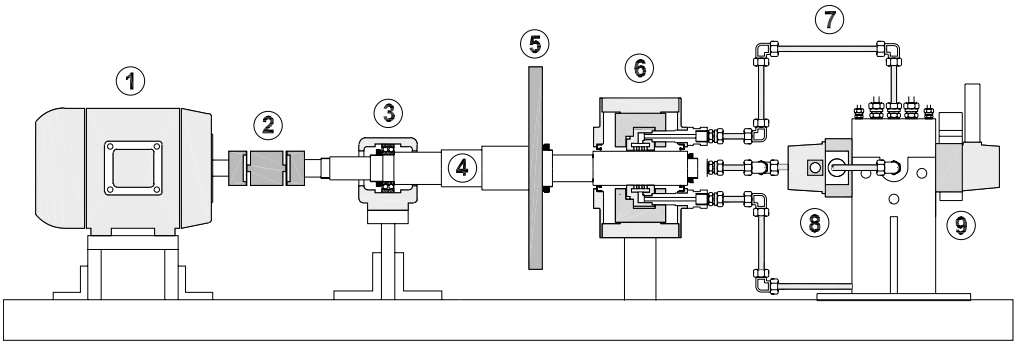

Fig. 3. Rotor-active bearing system: 1—electric motor ; 2—coupling ; 3—ball bearing ; 4—shaft ; 5—disk ; 6—active bearing ; 7—pipeline ; 8–9—servo valves.

and frequency responses, and the efficiency of the control system in reducing vibration is analysed. The theoretical study presented here is based on a test rig, which was constructed in the State University of Campinas, and is schematically shown in Fig. 3. The system characteristic data can be seen in Table 1. Experimental results will be presented in the near future.

2. Mathematical modelling of the rotor-bearing system

2.1. Rigid rotor

The rotor of the system studied in this work consists of a shaft and a disk (Fig. 3). This shaft disk sub-system is considered rigid in the frequency range of study (0–80 Hz). Therefore, one can determine four points in the shaft upon which external forces act: the coupling point, where the driving torque is applied (point A); the ball bearing position (point R); the rotor centre of gravity position (point O); and the active tilting-pad bearing position (point H)—see Figs. 3 and 4.

Table 1
Rotor-bearing and hydraulic system characteristic data

Parameter	Symbol	Value	Unit
Distance from A to R	r_{AR}	0.1360	m
Distance from R to O	r_{RO}	0.2078	m
Distance from R to H	r_{RH}	0.3740	m
Distance from R to disk	r_{RD}	0.2215	m
Shaft polar moment	I_{xx}	0.2038	kg.m^2
Shaft lateral moment	I_{yy}, I_{zz}	0.2981	kg m^2
Shaft radius (point H)	R	0.0250	m
Pad polar moment	I_s	2.57×10^{-4}	kg m^2
Assembled clearance	h_0	150.0	μm
Pre-load factor	m_p	0.150	
Oil dynamic viscosity at 40°	μ	0.027	N s/m^2
Oil compressibility factor	β_f	8.0×10^8	N/m^2
Pipeline length	l_T	0.500	m
Pipeline diameter	d_T	0.001	m
Pipeline inner volume	V_0	3.93×10^{-7}	m^3
Servo valve input signal range	u_{min}^{max}	± 0.25	V
Servo valve eigenfrequency	ω_V	320.0	Hz
Servo valve damping factor	ξ_V	0.48	
Servo valve gain	K_V	8.91×10^{-6}	m^3/s V
Linearization coefficient (experimental)	K_{PQ}	1.13×10^{-12}	m^3/s Pa

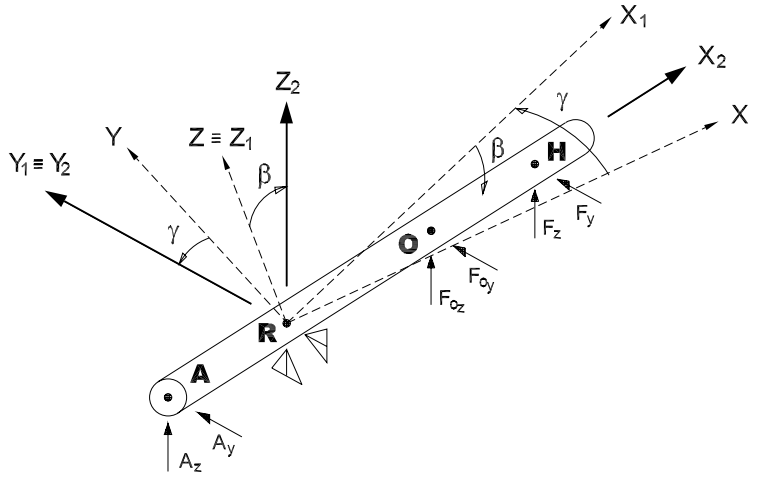

Fig. 4. Points of acting forces (A, R, O, H) and auxiliary reference frames used in the rigid model of the shaft-disk subsystem.

In Fig. 4, A_y and A_z are the coupling forces, F_{O_y} and F_{O_z} are the external forces applied to the rotor centre of mass, and F_y and F_z are the hydrodynamic forces of the active tilting-pad bearing.

By using auxiliary reference frames, one can describe the shaft angular displacements (ϕ, β and γ) around point R by following consecutive Kardan rotations: firstly around Z (inertial reference

frame), secondly around Y_1 (auxiliary reference frame $B1$) and finally around X_2 (auxiliary reference frame $B2$, attached to the shaft as illustrated in Fig. 4). By applying Euler's equation, considering the linear acceleration of point R as zero, one achieves the non-linear *equations of motion of the rigid rotor*:

$$\ddot{\beta} = \frac{1}{I_{yy}}\left[(I_{xx} - I_{zz})\dot{\gamma}^2 \sin\beta\cos\beta + \left(r_{AR}F_{A_y} - r_{RO}F_{O_y} - r_{RH}F_y\right)\sin\beta\sin\gamma - I_{xx}\dot{\phi}\dot{\gamma}\cos\beta + \left(r_{AR}F_{A_z} - r_{RO}F_{O_z} - r_{RH}F_z\right)\cos\beta + M_\beta\right],$$

$$\ddot{\gamma} = \frac{1}{I_{zz}\cos\beta}\left[\left(I_{yy} + I_{zz} - I_{xx}\right)\dot{\beta}\dot{\gamma}\sin\beta + I_{xx}\dot{\phi}\dot{\beta} + \left(-r_{AR}F_{A_y} + r_{RO}F_{O_y} + r_{RH}F_y\right)\cos\gamma + M_\gamma\right] \quad (1)$$

In Eq. (1), the rotor spin $\dot{\phi}$ is a known parameter, M_β and M_γ are external moments (excitation), r_{AR} is the distance between points A and R, r_{RO} is the distance between points R and O, r_{RH} is the distance between points R and H, and I_{xx}, I_{yy}, and I_{zz} are the polar and lateral moments of inertia of the shaft, in reference to point R.

2.2. Active tilting-pad bearing

The active bearing is composed of four tilting pads: two in the horizontal and two in the vertical directions (Y- and Z-axis of the inertial reference frame—Fig. 1). The *equation of motion of the* ith *pad* can be written as

$$I_s\ddot{\alpha}_i = M_{\alpha_i}, \quad (2)$$

where I_s is the pad rotational inertia, α_i is the tilting angular displacement of the ith pad around its pivot, and M_{α_i} is the resultant moment of the hydrodynamic forces in the i-th pad.

The hydrodynamic forces are calculated by integrating the oil pressure distribution over each pad surface area (Fig. 5(a)) and decomposing it into normal and tangential forces (Fig. 5(b)),

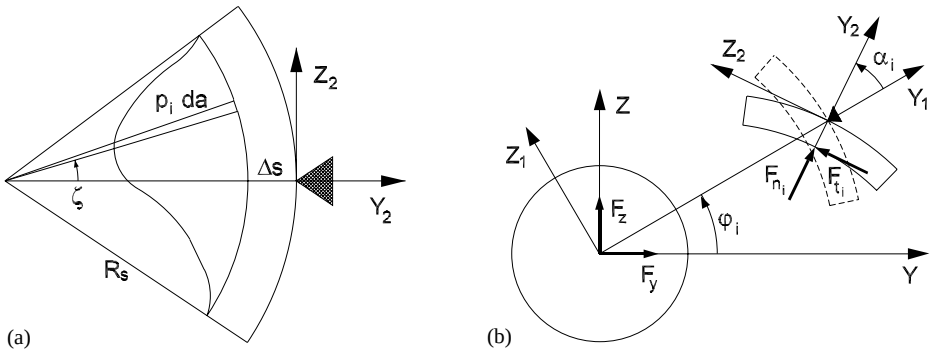

Fig. 5. Integration of forces acting on the ith pad and on the shaft: (a) integration of hydrodynamic pressure distribution on the pad; (b) force components acting on the pad and on the shaft.

as follows:

$$F_{n_i} = \int_a p_i \cos\zeta \, \mathrm{d}a, \qquad F_{t_i} = \int_a p_i \sin\zeta \, \mathrm{d}a,$$

where F_{n_i} is the hydrodynamic force acting perpendicular to the pad surface, F_{t_i} is the hydrodynamic force acting tangential to the pad surface, p_i is the oil pressure in the gap between the rotor and the ith pad, and ζ is the angle of curvature of the pad.

Thus, the resultant moment of the hydrodynamic forces on pads is given by

$$M_{\alpha_i} = -F_{t_i}\Delta_s,$$

where Δ_s is the distance between the pad surface and its pivoting point (Fig. 5(a)). The hydrodynamic forces F_y and F_z, acting on the shaft, are calculated by projecting the hydrodynamic forces acting on the four bearing pads into the directions Y and Z, considering the angular position of each pad (α_i):

$$F_y = -\sum_{i=1}^{4}\left[F_{n_i}\cos(\varphi_i+\alpha_i) - F_{t_i}\sin(\varphi_i+\alpha_i)\right],$$

$$F_z = -\sum_{i=1}^{4}\left[F_{n_i}\sin(\varphi_i+\alpha_i) + F_{t_i}\cos(\varphi_i+\alpha_i)\right],$$

where φ_i is the angular position of the ith pad pivot around the bearing housing (Fig. 5(b)).

The oil pressure distribution is obtained by solving numerically the modified Reynolds' equation

$$\frac{\partial}{\partial\bar{x}}\left(\frac{h_i^3}{\mu}\frac{\partial p_i}{\partial\bar{x}}\right) + \frac{\partial}{\partial\bar{z}}\left(\frac{h_i^3}{\mu}\frac{\partial p_i}{\partial\bar{z}}\right) - \frac{3}{\mu l_0}\mathscr{F}(\bar{x},\bar{z})\,p_i = 6U\frac{\partial h_i}{\partial\bar{z}} + 12\frac{\partial h_i}{\partial t} - \frac{3}{\mu l_0}\mathscr{F}(\bar{x},\bar{z})P_i, \tag{3}$$

where h_i is the gap between the rotor and the ith pad, μ is the oil dynamic viscosity, l_0 is the orifice's length, U is the linear velocity of the rotor surface, P_i is the injection pressure in the ith pad (active lubrication), and $\mathscr{F}(\bar{x},\bar{z})$ is a positioning function of the orifices on the pad surface.

Eq. (3), and the previous expressions, have been thoroughly deduced in the work of Santos and Russo [9].

2.3. Hydraulic system

The hydraulic system consists of a reservoir, two pumps and two servo valves. One of the pumps supplies the conventional lubrication to the bearing. The second pump feeds the injection system with high pressurised oil. The purpose of the servo valves is to control the pressure at which oil is injected, through the pad bores, into the bearing gap (Fig. 2).

According to Thayer [16] and Rashidi and Dirusso [17], the dynamics of the oil flow through a servo valve may be described by a second order equation. For the two servo valves, they are

$$\begin{aligned}
&\ddot{Q}_{V_\mathrm{I}} + 2\,\xi_{V_\mathrm{I}}\omega_{V_\mathrm{I}}\dot{Q}_{V_\mathrm{I}} + \omega_{V_\mathrm{I}}^2 Q_{V_\mathrm{I}} = \omega_{V_\mathrm{I}}^2 K_{V_\mathrm{I}} u_\mathrm{I}(t),\\
&\ddot{Q}_{V_\mathrm{II}} + 2\,\xi_{V_\mathrm{II}}\omega_{V_\mathrm{II}}\dot{Q}_{V_\mathrm{II}} + \omega_{V_\mathrm{II}}^2 Q_{V_\mathrm{II}} = \omega_{V_\mathrm{II}}^2 K_{V_\mathrm{II}} u_\mathrm{II}(t),
\end{aligned} \tag{4}$$

where Q_V is the oil flow through the servo valve under null loading (open ducts), ξ_V is the damping factor of the servo valve, ω_V is the eigenfrequency of the servo valve, K_V is the gain of the servo valve, $u(t)$ is the control signal, and indices I and II identify the servo valves connected to the pads in the horizontal and vertical directions respectively.

The oil pressure in the ports of the servo valves is obtained by solving the following equations:

$$\frac{V_0}{\beta_f}\dot{P}_1 + \left(K_{PQ_{\mathrm{I}}} + \frac{\pi d_T^4}{128\mu l_T}\right)P_1 - K_{PQ_{\mathrm{II}}}\ P_3 - Q_{V_{\mathrm{I}}} = \frac{\pi d_T^4}{128\mu l_T}\bar{p}_1,$$

$$\frac{V_0}{\beta_f}\dot{P}_3 - K_{PQ_{\mathrm{I}}}\ P_1 + \left(K_{PQ_{\mathrm{I}}} + \frac{\pi d_T^4}{128\mu l_T}\right)P_3 + Q_{V_{\mathrm{I}}} = \frac{\pi d_T^4}{128\mu l_T}\bar{p}_3, \tag{5}$$

$$\frac{V_0}{\beta_f}\dot{P}_2 + \left(K_{PQ_{\mathrm{II}}} + \frac{\pi d_T^4}{128\mu l_T}\right)P_2 - K_{PQ_{\mathrm{II}}}P_4 - Q_{V_{\mathrm{II}}} = \frac{\pi d_T^4}{128\mu l_T}\bar{p}_2,$$

$$\frac{V_0}{\beta_f}\dot{P}_4 - K_{PQ_{\mathrm{II}}}P_2 + \left(K_{PQ_{\mathrm{II}}} + \frac{\pi d_T^4}{128\mu l_T}\right)P_4 + Q_{V_{\mathrm{II}}} = \frac{\pi d_T^4}{128\mu l_T}\bar{p}_4, \tag{6}$$

where P_i is the oil injection pressure in the ith pad, $\bar{p}_i$ is the average hydrodynamic pressure in the gap of the ith pad, K_{PQ} is an empirical constant, V_0 is the pipeline inner volume, β_f is the oil compressibility factor, and d_T and l_T are the diameter and length of the pipeline.

The constant K_{PQ} states the relationship between the oil flow through the servo valve and the pressure difference at its ports, when the control signal is null: $K_{PQ} = \partial Q/\partial \Delta P\big|_{u=0}$. It can be obtained experimentally by increasing the pressure difference at the ports of the servo valve and measuring the resultant oil flow.

Eqs. (4)–(6) represent a relationship between the control signal applied to each of the servo valves and the resultant injection pressures at their respective ports. They are obtained by applying a first order approximation, assuming laminar flow conditions in the pipeline, and considering the oil compressibility effects. The deduction of these equations is presented in detail in Nicoletti and Santos [15].

3. Control techniques

Eqs. (1), (2) and (4)–(6) form the set of non-linear equations of motion of the rotor-bearing system in study. Once the mathematical model of the system is deduced, one has to choose the control laws which will be used in the feedback. The laws of four different controllers are deduced below.

3.1. PI at maximum input signal

A *PI* controller is classically defined by the expression

$$u = K_p\, e + \frac{K_p}{T_i}\int e\,\mathrm{d}t, \tag{7}$$

where e is the error between the output and the reference signals, K_p is the proportional gain, and T_i is the integral time.

By differentiating Eq. (7) and writing it in a discrete form by finite differences, one has

$$\dot{u} = K_p\dot{e} + \frac{K_p}{T_i}e \Rightarrow \frac{u-u^*}{T} = K_p\frac{e-e^*}{T} + \frac{K_p}{T_i}e \Rightarrow u = u^* + K_p\left(e-e^*\right) + K_i\, e, \tag{8}$$

where u is the control signal at a certain instant of time, u^* is the last sample value of the control signal (instant $t-T$), e^* is the last sample error, T is the sampling period, and K_i is the integral gain ($K_i = K_pT/T_i$).

The error is given by the difference between the actual shaft position and the desired shaft position. For the two directions in the rotor-bearing system, one has

$$e_Y = Y - Y_R, \qquad e_Z = Z - Z_R, \tag{9}$$

where Y_R and Z_R are the reference values of shaft position.

Hence, by inserting Eq. (9) into Eq. (8), one arrives to the *PI* control laws for the two servo valves, as follows:

$$\begin{aligned} u_{\mathrm{I}}(t) &= u_{\mathrm{I}}^* K_p\left[(Y-Y_R) - \left(Y^*-Y_R\right)\right] + K_i(Y-Y_R),\\ u_{\mathrm{II}}(t) &= u_{\mathrm{II}}^* K_p\left[(Z-Z_R) - \left(Z^*-Z_R\right)\right] + K_i(Z-Z_R), \end{aligned} \tag{10}$$

where Y and Z are the linear shaft displacements at point H ($Y = r_{RH}\gamma$, $Z = -r_{RH}\beta$), and Y^* and Z^* are the last sample values of these displacements.

In order to apply Eq. (10) to the problem in study, the gains were chosen to have maximum control signal ($u = 0.25\,\mathrm{V}$) when the error is maximum (Y or $Z \equiv h_0 = 150\,\mu\mathrm{m}$)—see system characteristics in Table 1. Since this occurs for $K_p = 1667\,\mathrm{V/m}$ and $K_i = 5\,\mathrm{V/m}$, the *PI control law at maximum input signal* is thus given by

$$\begin{aligned} u_{\mathrm{I}}(t) &= u_{\mathrm{I}}^* + 1667\left(Y - Y^*\right) + 5\,Y,\\ u_{\mathrm{II}}(t) &= u_{\mathrm{II}}^* + 1667\left(Z - Z^*\right) + 5\,Z, \end{aligned} \tag{11}$$

where one assumes as reference the bearing centre ($Y_R = Z_R = 0$).

3.2. PD upon system linearization

Assuming that the rotor displacements are small ($\sin\beta \approx \beta$, $\cos\beta \approx 1$, $\sin\gamma \approx \gamma$, $\cos\gamma \approx 1$ and $\dot{\gamma}^2\beta$, $\dot{\beta}\dot{\gamma}\beta$ and $\beta\gamma$ negligible) one can linearise the equations of motion (Eqs. (1), (2) and (4)–(6)) in order to calculate the *PD* controller gains. Thus, the equations of motion of the bearing system can be written in the form

$$\mathbf{I}\,\ddot{\psi} + \mathbf{G}(\dot{\phi})\,\dot{\psi} = \mathbf{M}_h + \mathbf{M}_e, \tag{12}$$

where $\mathbf{I}$ is the inertia matrix, $\mathbf{G}(\dot{\phi})$ is the gyroscopic matrix, $\mathbf{M}_h$ is the vector of hydraulic moments, $\mathbf{M}_e$ is the vector of external moments, and ψ is the vector of angular displacements ($\psi = \{\,\beta\ \gamma\,\}^{\mathrm{T}}$).

The vector of hydraulic moments can be decomposed into a vector of linearised moments caused by the oil film (hydrodynamic forces) and a vector of linearised moments caused by the oil injection (hydrostatic forces – hydraulic system). Hence, one has

$$\mathbf{M}_h = \{\ -\mathbf{D}\,\dot{\mathbf{q}} - \mathbf{K}\,\mathbf{q}\,\} + \{\boldsymbol{\Lambda}\,\mathbf{u}\}, \tag{13}$$

where **D** and **K** are the damping and stiffness matrices of the oil film, **q** is the vector of linear displacements of the rotor ($\mathbf{q} = \{Y\ Z\}^{\mathrm{T}}$), **u** is the control vector ($\mathbf{u} = \{u_{\mathrm{I}}\ u_{\mathrm{II}}\}^{T}$), and **Λ** is the matrix which correlates the control vector with the resultant hydrostatic forces from the injection (numerically obtained).

By using the relationships between angular and linear displacements of the shaft at point H:

$$Y = r_{RH}\gamma, \qquad Z = -r_{RH}\beta, \tag{14}$$

one can insert Eq. (13) into Eq. (12). Rearranging it, one arrives to the state formulation of the problem:

$$\dot{\Psi} = \mathbf{A}\,\Psi + \mathbf{B}\,\mathbf{u} + \eta_e. \tag{15}$$

By applying a state feedback control vector of the form

$$\mathbf{u} = -\mathbf{H}\,\Psi, \tag{16}$$

and neglecting the state vector of external moments (η_e), from Eq. (15) one has

$$\dot{\Psi} = (\mathbf{A} - \mathbf{BH})\Psi = \mathbf{L}\,\Psi. \tag{17}$$

By giving a set of desired eigenvalues, which will be the desired system eigenvalues, one has the desired coefficients of the characteristic equation of **L**. The gain matrix **H** can be determined by comparing the coefficients of the characteristic equation of **L** to those desired ones. If the gain matrix **H** is a full matrix (coupled control signals), then the solution is not unique and different gain matrices may lead to similar results [18,19]. In this work, the control signals are assumed to be uncoupled ($u_{\mathrm{I}} = u_{\mathrm{I}}(\dot{\gamma}, \gamma)$ and $u_{\mathrm{II}} = u_{\mathrm{II}}(\dot{\beta}, \beta)$), thus making the gain matrix unique.

The stiffness (**K**) and damping (**D**) matrices of the oil film are calculated considering that the additional radial injection is also taking place, based on the differential principle of the servo valves. In other words, setting the geometric and operational condition of the rotor-bearing system (Sommerfeld number S), the equilibrium position of the rotor-bearing system in a certain direction (eccentricity ε) is altered by statically changing the injection pressure in the pads mounted in this direction (pads #1 and #3 for Y direction and pads #2 and #4 for Z direction—Fig. 1). Therefore, in this case, the equilibrium position is also function of the control signal, which dictates the injection pressure in the pads ($\varepsilon_y = \varepsilon_y(u_I)$, $\varepsilon_z = \varepsilon_z(u_{\mathrm{II}})$). For each new equilibrium position, the rotor-bearing system is perturbed, and stiffness and damping coefficients are calculated by the formulation proposed by Springer [20], by choosing a condensation (or excitation) frequency ω.

Fig. 6 illustrates the dependency of the coefficients K_{yy}, K_{zz}, D_{yy}, D_{zz} and of the equilibrium position in the Z direction (ε_z) on Sommerfeld number and control signal u_{II}, for the hybrid lubrication case. It is important to point out that **K** and **D** are also a function of frequency ω. An excitation frequency of 80 Hz was used since this is the maximum frequency in the range of study in this work.

Hence, for a rotating frequency of 30 Hz ($S = 0.2576$), control signal $u_{\mathrm{II}} = 0\ V$, an excitation frequency of 80 Hz, and considering the rotor weight (the case in study), the oil film coefficients

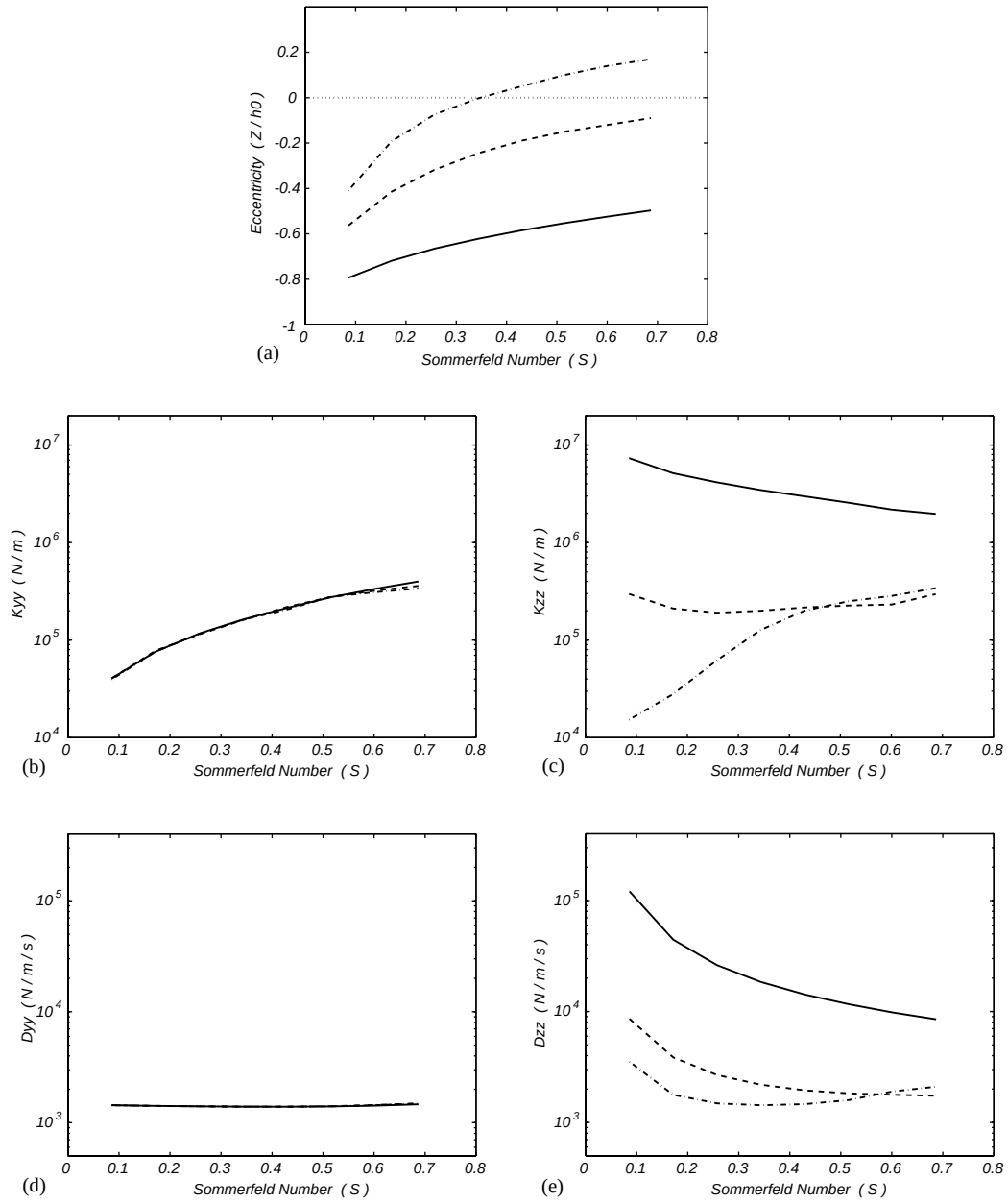

Fig. 6. Eccentricity (ε_z) and dynamic coefficients as a function of the Sommerfeld number and control signal u_{II} in the direction of static loading (weight in the Z direction, excitation frequency $\omega = 80\,\mathrm{Hz}$, $u_I = 0\,\mathrm{V}$, $\varepsilon_y \approx 0$): (a) eccentricity in the Z direction; (b) stiffness in the Y direction; (c) stiffness in the Z direction; (d) damping in the Y direction; (e) damping in the Z direction; —— , $u_{\mathrm{II}} = 0\,\mathrm{V}$; – – – , $u_{\mathrm{II}} = -0.1\,\mathrm{V}$; – · – , $u_{\mathrm{II}} = -0.11\,\mathrm{V}$.

are as follows:

$$K_{yy} \approx 1.2 \times 10^5 \text{ N/m}, \quad D_{yy} \approx 1.4 \times 10^3 \text{ N/(m/s)},$$
$$K_{zz} \approx 4.1 \times 10^6 \text{ N/m}, \quad D_{zz} \approx 2.6 \times 10^4 \text{ N/(m/s)},$$
$$K_{yz} \approx K_{zy} \approx \mathcal{O}(10^3), \quad D_{yz} \approx D_{zy} \approx \mathcal{O}(10^1).$$

Matrix $\boldsymbol{\Lambda}$ is obtained numerically and, for the case in study, given by

$$\boldsymbol{\Lambda} = \begin{bmatrix} -1176.4 & 0 \\ 0 & -1176.4 \end{bmatrix}.$$

Using the procedure described above, by choosing the set of eigenvalues: $s_1 = -1000$, $s_2 = -900$, $s_3 = -800$, and $s_4 = -700$, in order to achieve an over-damped system, one arrives to the gain matrix

$$\mathbf{H} = \begin{bmatrix} 0 & 0.61979 & 0 & 444.44 \\ -0.79368 & 0 & -443.18 & 0 \end{bmatrix}$$

which results in PD control laws of the form:

$$u_{\mathrm{I}}(t) = 0.61979\dot{\gamma} + 444.44\gamma, \quad u_{\mathrm{II}}(t) = -0.79368\dot{\beta} - 443.18\beta. \tag{18}$$

Using expression (14), one arrives at the *PD control law obtained upon system linearization*, as follows:

$$u_{\mathrm{I}}(t) = 1.657\,\dot{Y} + 1188.34\,Y, \quad u_{\mathrm{II}}(t) = 2.122\,\dot{Z} + 1184.97Z. \tag{19}$$

3.3. PID upon system linearization

The *PID* controller is classically defined as

$$u = K_d\dot{e} + K_p e + \frac{K_p}{T_i}\int e\,\mathrm{d}t, \tag{20}$$

where K_d is the derivative gain.

Differentiating expression (20), and writing it in a discrete form by using finite differences similarly to Eq. (8), one has

$$\dot{u} = K_d\,\ddot{e} + K_p\,\dot{e} + \frac{K_p}{T_i}e \Rightarrow \frac{u-u^*}{T} = K_d\,\frac{\dot{e}-\dot{e}^*}{T} + K_p\,\frac{e-e^*}{T} + \frac{K_p}{T_i}e$$
$$\Rightarrow u = u^* + K_d\left(\dot{e}-\dot{e}^*\right) + K_p\left(e-e^*\right) + K_i\,e. \tag{21}$$

Inserting expressions (9) into Eq. (21), one has for the two servovalves:

$$u_{\mathrm{I}}(t) = u_{\mathrm{I}}^* + K_d(\dot{Y} - \dot{Y}^*) + K_p\left(Y - Y^*\right) + K_i\,Y,$$
$$u_{\mathrm{II}}(t) = u_{\mathrm{II}}^* + K_d\,(\dot{Y} - \dot{Y}^*) + K_p\left(Z - Z^*\right) + K_i Z. \tag{22}$$

By using the gain calculated in the previous section, and inserting the integral term, one arrives at the *PID control law* as follows:

$$u_{\mathrm{I}}(t) = u_I^* + 1.657(\dot{Y} - \dot{Y}^*) + 1188.34(Y - Y^*) + 5Y,$$
$$u_{\mathrm{II}}(t) = u_{\mathrm{II}}^* + 2.122(\dot{Z} - \dot{Z}^*) + 1184.97(Z - Z^*) + 5Z, \tag{23}$$

where one assumes as reference the bearing centre ($Y_R = Z_R = 0$).

3.4. Non-linear proportional control

In the active bearing in study, the shaft positions (Y and Z) depend non-linearly on the control signal $u(t)$. In the case of null external forces, this non-linear relationship can be computed by simply varying the control signal, and observing the resultant shaft displacements, for a given rotating frequency $\dot{\phi}$. Thus, one can arrive at expressions in the form:

$$Y = Y(u_I, \dot{\phi}), \quad Z = Z(u_{\mathrm{II}}, \dot{\phi}).$$

When the shaft presents a certain displacement due to the application of a given control signal, it means that the hydrostatic and hydrodynamic forces in the bearing, due to the oil injection (control system), are acting on the shaft and forcing it to the resultant position. Therefore, one can infer that one can centre the shaft in the bearing by applying the same forces on the opposite direction. This can be done by using the inverse relationship between the displacements and the control signals:

$$u_{\mathrm{I}} = u_{\mathrm{I}}(Y, \dot{\phi}), \quad u_{\mathrm{II}} = u_{\mathrm{II}}(Z, \dot{\phi}).$$

Hence, for a given shaft position (Y,Z), one can use the inverse relationships as non-linear control laws to calculate the necessary input signals to the servo valves. As a result, the hydrostatic forces of the injection system will compensate the forces acting on the shaft, and locate the shaft back to the bearing centre.

For a rotating frequency of 30 Hz and using the system parameters shown in Table 1, one arrives at the following *non-linear proportional control laws*:

$$u_{\mathrm{I}}(t) = 3.1 \times 10^4 Y^5 - 4.17 \times 10^2 Y^3 + 1.54Y,$$

$$u_{\mathrm{II}}(t) = 3.1 \times 10^4 Z^5 - 4.17 \times 10^2 Z^3 + 1.54Z, \tag{24}$$

where the coefficients of expression (24) are given in V/mm^5, V/mm^3 and V/mm respectively, and were obtained by using interpolation routines of software MATLAB®.

4. Numerical results

The system of equations of motion (Eqs. (1), (2) and (4)–(6)) is integrated in the time domain with help of the software MATLAB®. The modified Reynolds' equation (3) is also solved and the pressure distribution integrated by using this software. For that, a two-dimensional uniform grid is created over each pad surface and composed of 42 points in the tangential direction (direction of shaft rotation) and 31 points in the axial direction of shaft, where central approximations of the

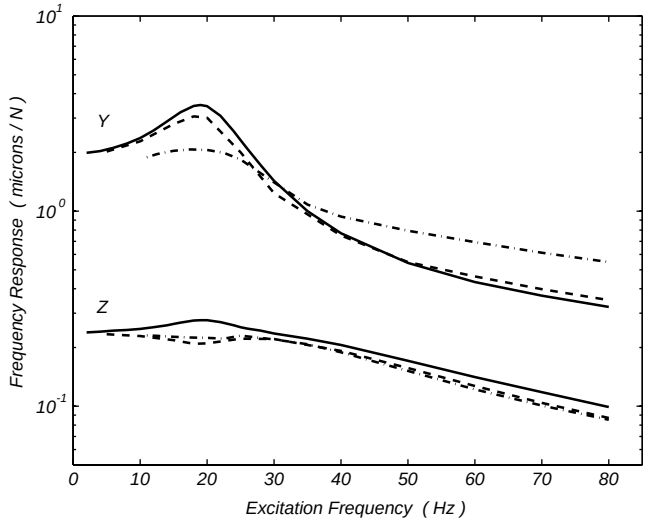

Fig. 7. FRFs of the passive system (peak-to-peak)—quasi-linear and non-linear behaviours ($\dot{\phi} = 30$ Hz, $S = 0.2576$): —— , $F_e = 1$ N; – – – , $F_e = 10$ N; – · – , $F_e = 50$ N.

finite difference method are applied. The parameter values used in the numerical simulations of the active system are shown in Table 1.

4.1. Frequency response

In the case of external excitation, the exciting moments are given as

$$M_\beta = -F_e e_x \sin(\omega t), \quad M_\gamma = F_e e_x \cos(\omega t),$$

where F_e is the force amplitude, e_x is the distance between the origin (point R—Fig. 4) and the force application point, and ω is the excitation frequency. For the case in study, $e_x = r_{RD}$ (excitation is applied to the disk position in the shaft).

Fig. 7 shows the peak-to-peak frequency response functions (FRFs) of the passive system (injection system turned off), running at a rotating frequency of 30 Hz and subjected to shaft weight (Sommerfeld number $S = 0.2576$), for dynamic excitation loads of 1, 10 and 50 N. As one can see, for small amplitudes of excitation (between 1 and 10 N), the system may be considered almost linear (similar FRFs), characterized by large displacements in the Y direction (horizontal) and small displacements in the Z direction (vertical). The small displacements in the Z direction are caused by the static loading (weight), which forces the rotor towards the pad, thus diminishing the gap and increasing the damping in this direction (Fig. 6).

For the case of an excitation of 50 N, the frequency response changes, showing a more damped system behaviour (lower values at resonance, both in the Y and Z directions—Fig. 7). This is caused by the increase of exciting force, which results in a decrease of the bearing gap between the rotor and the pads, thus rising the damping and affecting the response. Hence, the performance of the linear and non-linear controllers (Eqs. (11), (19), (23) and (24)) are investigated for the cases of 1 and 50 N of excitation amplitude, where the system non-linearities are more evident.

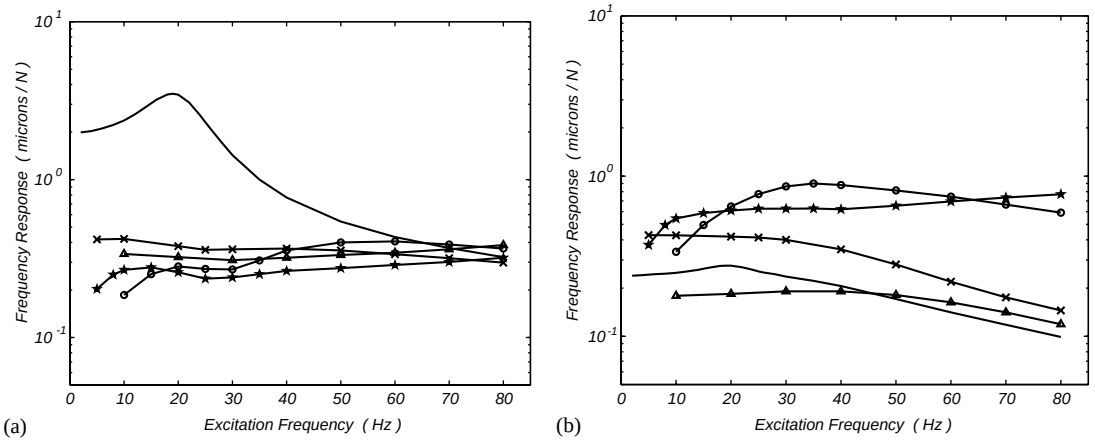

Fig. 8. FRFs of the passive and active systems (peak-to-peak)—Quasi-linear behaviour ($F_e = 1$ N, $\dot{\phi} = 30$ Hz, $S = 0.2576$): (a) Y direction (horizontal); (b) Z direction (vertical); —— , passive; –★– , PI; –×– , PD; –○– , PID; –△– , non-linear P.

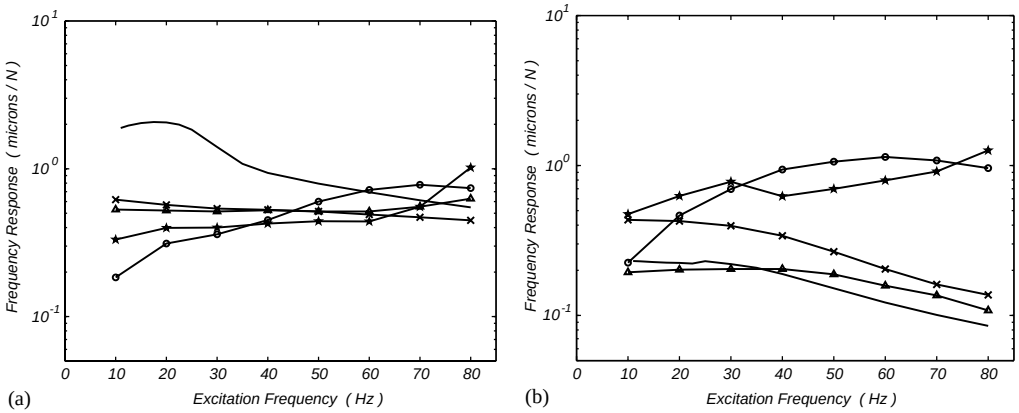

Fig. 9. FRFs of the passive and active systems (peak-to-peak)—non-linear behaviour ($F_e = 50$ N, $\dot{\phi} = 30$ Hz, $S = 0.2576$): (a) Y direction (horizontal); (b) Z direction (vertical); —— , passive; –★– , PI; –×– , PD; –○– , PID; –△– , non-linear P.

Figs. 8 and 9 show the FRFs obtained by using the active bearing system under the deduced control laws. For both cases of excitation ($F_e = 1$ and 50 N), all the control strategies managed to reduce vibration amplitudes sensibly in the Y direction (horizontal), keeping the amplitudes in the Z direction (vertical) at small values. This vibration amplitude reduction is remarkable near system resonance, at 20 Hz (Y direction), although, at higher exciting frequencies (above 60 Hz), some of the controllers presented a worse performance compared to the passive case.

By analysing the results in the Z (vertical) direction, one can see that the controller performances were not as efficient as those obtained in the Y (horizontal) direction. One has achieved higher amplitude responses compared to the passive case, being the proportional non-linear controller, the only one to reduce vibration at the resonance in this direction, in both cases of excitation (1 and 50 N). The use of the PD controller resulted to response amplitudes of the

same order of those obtained in the Y direction and, additionally, a tendency to present response values near to those of the passive case at higher frequencies. Controllers PI and PID presented poorer performances in the Z direction, with higher amplitude responses compared to those obtained in the Y direction.

This worse performance of the active system in the Z direction can be explained by analysing the rotor equilibrium position in the bearing, resulted from the control strategies (Table 2). In the passive case, the rotor presents a certain eccentricity in the bearing due to the static loading (weight). As a consequence, the bearing gap in the loading direction is decreased, thus enhancing the damping (see Fig. 6). This fact explains the difference of amplitude responses in the Y and Z directions for the passive case, in Fig. 7. The worse controllers in this frequency response analysis are those which eliminate the rotor eccentricity in the bearing (see Table 2). The PI and PID controllers centre the shaft in the bearing, whereas the other controllers do not. The fact of suppressing rotor eccentricity tends to decrease the bearing damping in the direction of this eccentricity (see Fig. 6(e)). In fact, the lowest damping level is achieved when the rotor is centred in the bearing (see Figs. 6(a) and (e)). As a result, this damping reduction has to be overcome by the controllers. In this study, the proposed PI and PID controllers were not robust enough to recover the damping loss due to the rotor centring. Thus, the resulted response was higher than that of the passive case. The PD and non-linear P controllers had a better performance in the Z direction, since there was still some rotor eccentricity in the bearing (Table 2). As a matter of fact, the non-linear P controller, which had the best performance in reducing vibration in the Z direction (Figs. 8 and 9), is the one that presented the largest rotor eccentricity among those studied strategies.

Hence, for the adopted conditions and frequency range of study, the proposed PD and the non-linear P controllers are better suited to reduce vibration in the considered rotating system, with help of an active hybrid bearing. However, it is important to note that the control laws with integral terms (PI and PID) may also lead to satisfactory results whenever the control system has enough power to supply to the system, in order to overcome the damping loss due to rotor centring.

4.2. Unbalance response and instability

In the case of an unbalanced system, the exciting moments are given as

$$M_\beta = m_e e_x e_y \left(\ddot{\phi}\cos\phi - \dot{\phi}^2 \sin\phi\right),$$

$$M_\gamma = m_e e_x e_y \left(\ddot{\phi}\sin\phi + \dot{\phi}^2 \cos\phi\right),$$

Table 2
Rotor equilibrium positions resulted from the control strategies in study

Controller		Passive	PI	PD	PID	Non-linear P
Rotor eccentricity	Y/h_0	~ 0	~ 0	~ 0	~ 0	~ 0
	Z/h_0	-0.59	~ 0	-0.45	~ 0	-0.60

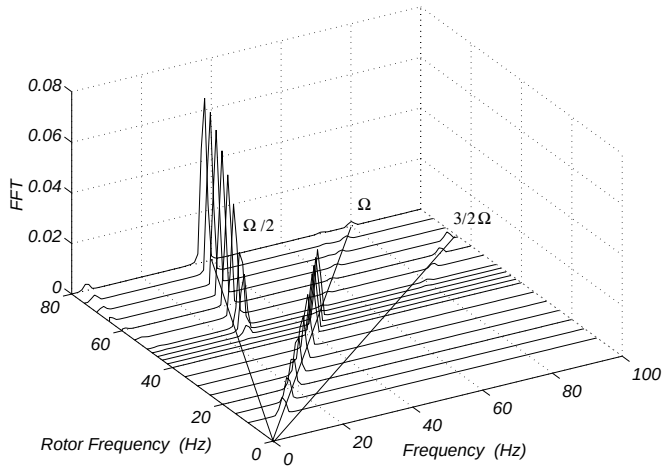

Fig. 10. Waterfall diagram of unbalance response—passive case under null static loading.

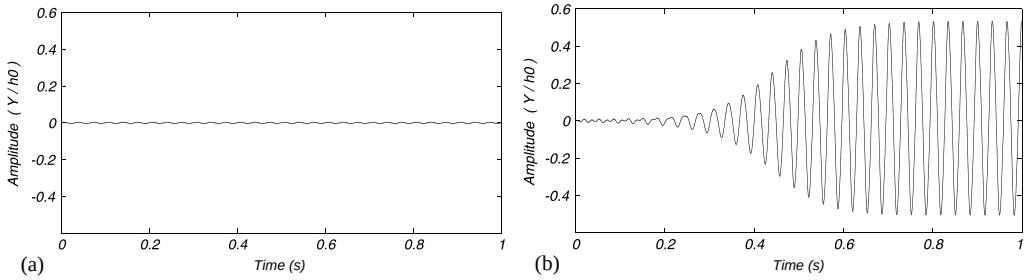

Fig. 11. Time response of the passive system under unbalance—*whirl* phenomenon at 60 Hz: (a) $\dot{\phi} = 30$ Hz; (b) $\dot{\phi} = 60$ Hz.

where m_e is the unbalance lumped mass, and e_x and e_y are the co-ordinates of the unbalance in reference to the shaft.

For the case in study and an unbalance in the disk position, one has $m_e = 5g \quad e_x = r_{RD}, \quad e_y = 5$ mm.

Hence, for the passive case (no control action), under null static loading (high Sommerfeld number condition), one achieves the system unbalance response shown in Fig. 10.

In Fig. 10, the system clearly vibrates at a synchronous frequency (typical of unbalanced systems), until the value of 47 Hz is reached. Beyond this limit, the system presents *whirl* instability, at a sub-synchronous frequency near half the rotating frequency, with remarkable increase of vibration amplitude. Fig. 11 shows the behaviour of the shaft in the time domain for rotating frequencies of 30 Hz (below stability limit) and 60 Hz (above stability limit), where the increase in vibration amplitude can be readily seen.

Whirl and whip instability in hydrodynamic bearings is extensively discussed in the literature, among other works in Muszynska [21]. In the case of tilting-pad bearings, it has been always believed that tilting-pad bearings were unconditionally stable, since they do not present cross-coupling effects. However, experimental results showed that this kind of bearing is not free from instability phenomena (mainly whirl instability), under certain operational conditions [22,23]. According to literature, these conditions are low pre-load factor and low static loading [24,25]. In the numerical simulations presented in this section, the pre-load factor is low ($m_p = 0.15$) and the static loading is null, thus being propitious conditions for the appearance of instability phenomena. It is interesting to highlight that static bearing loading close to zero can occasionally happen in radial compressors due to disposition of intake, and discharge and aerodynamic effects.

The solution to these instability problems is simply a matter of changing operational conditions by increasing the pre-load or the static loading. However, when it is not possible, it is interesting to investigate the performance of the rotor-bearing system, operating with a bearing lubricated actively, in such an adverse condition. Hence, by applying the control laws deduced in this work and the active bearing under study, one achieves the unbalance responses of the system under the same operational conditions of the passive case, as shown in Fig. 12.

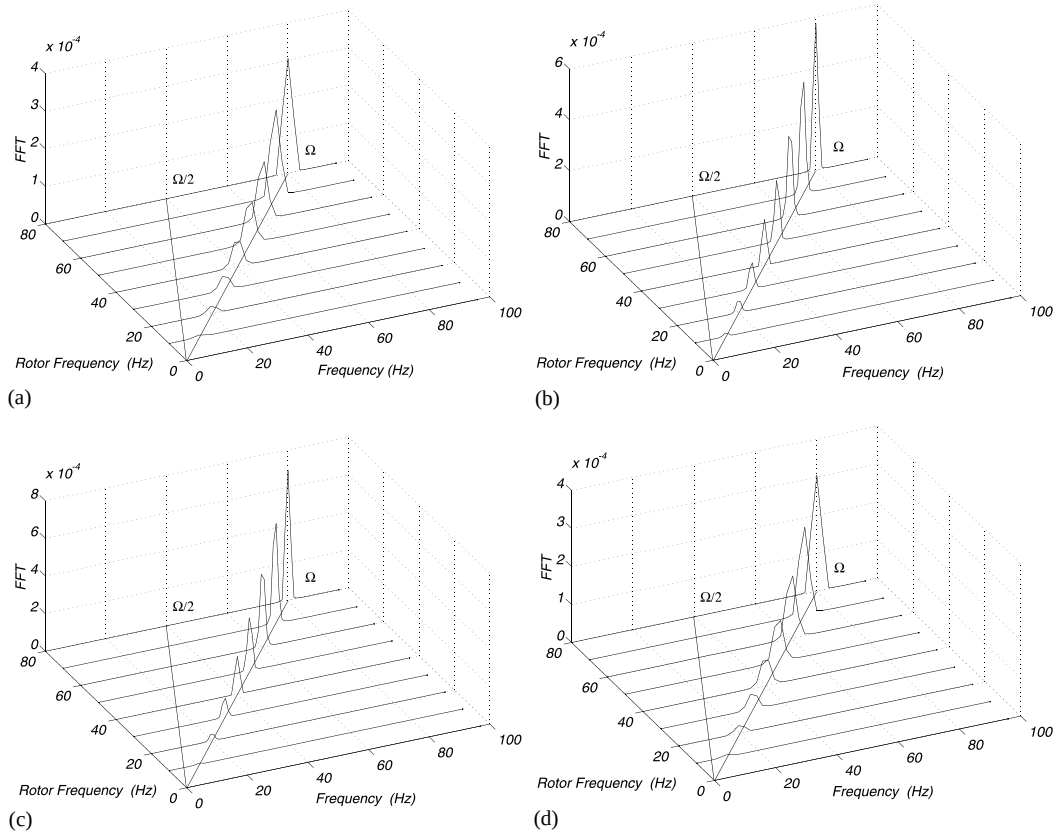

Fig. 12. Unbalance response functions of the active systems—null static loading: (a) PI; (b) PD; (c) PID; (d) non-linear P.

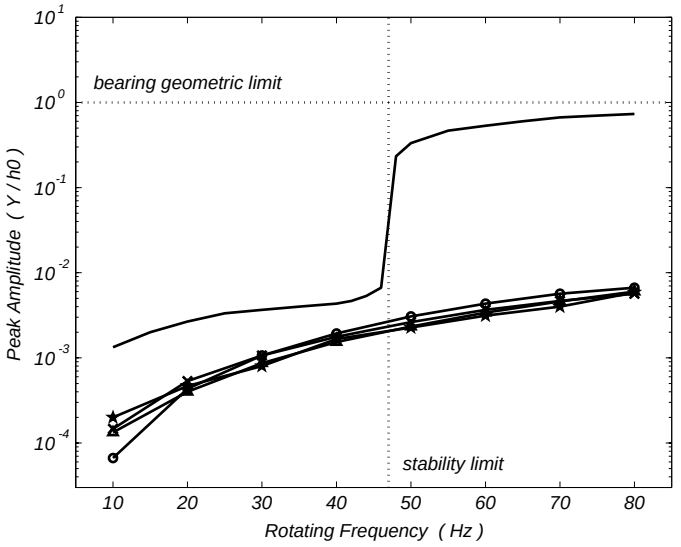

Fig. 13. Peak amplitudes as function of rotating frequency—unbalance response—passive and active cases: —— , passive; –★– , PI; –×– , PD; –○– , PID; –△– , non-linear P.

As can be seen in Fig. 12, the whirl components in the unbalance response are eliminated by using all the controllers under study. As a consequence, the system vibrates at the synchronous frequency, even for frequencies above 47 Hz, which indicates that the stability limit was shifted to a higher value by the control action of the bearing. By comparing the amplitude responses (Fig. 13), one can see this shift of the stability limit in the active cases, since rotor vibration remained under reasonable limits above the rotating frequency of 47 Hz.

Fig. 14 shows the rotor vibration in time domain for the cases of rotating frequencies of 30 and 60 Hz, under passive and active conditions. The control system was activated at the instant $t = 0.5$ s, or if the rotor amplitude (Y/h_0 or Z/h_0) reached values above ± 0.2. The elimination of whirl instability by the active system can be easily seen in Fig. 14, for the rotating frequenciy of 60 Hz, and vibration reduction is also achieved for the rotating frequency of 30 Hz. In general, all the controllers managed to reduce rotor vibration successfully, in the frequency range of study, being activated at $t = 0.5$ s, or if the amplitude (Y/h_0 or Z/h_0) was above ± 0.2.

5. Conclusion and future aspects

The active tilting-pad bearing with oil injection through the pads was presented and modelled. Some linear and non-linear control techniques were adopted and their respective control laws were deduced. The performances of the controllers in reducing rotor vibration are compared through unbalance and frequency response analyses.

In the unbalance response analysis, all the studied controllers managed to reduce significantly rotor vibration. The whirl instability which occurred in the system, due to the adopted operational conditions (high Sommerfeld number, low pre-load factor and low static loading), was eliminated

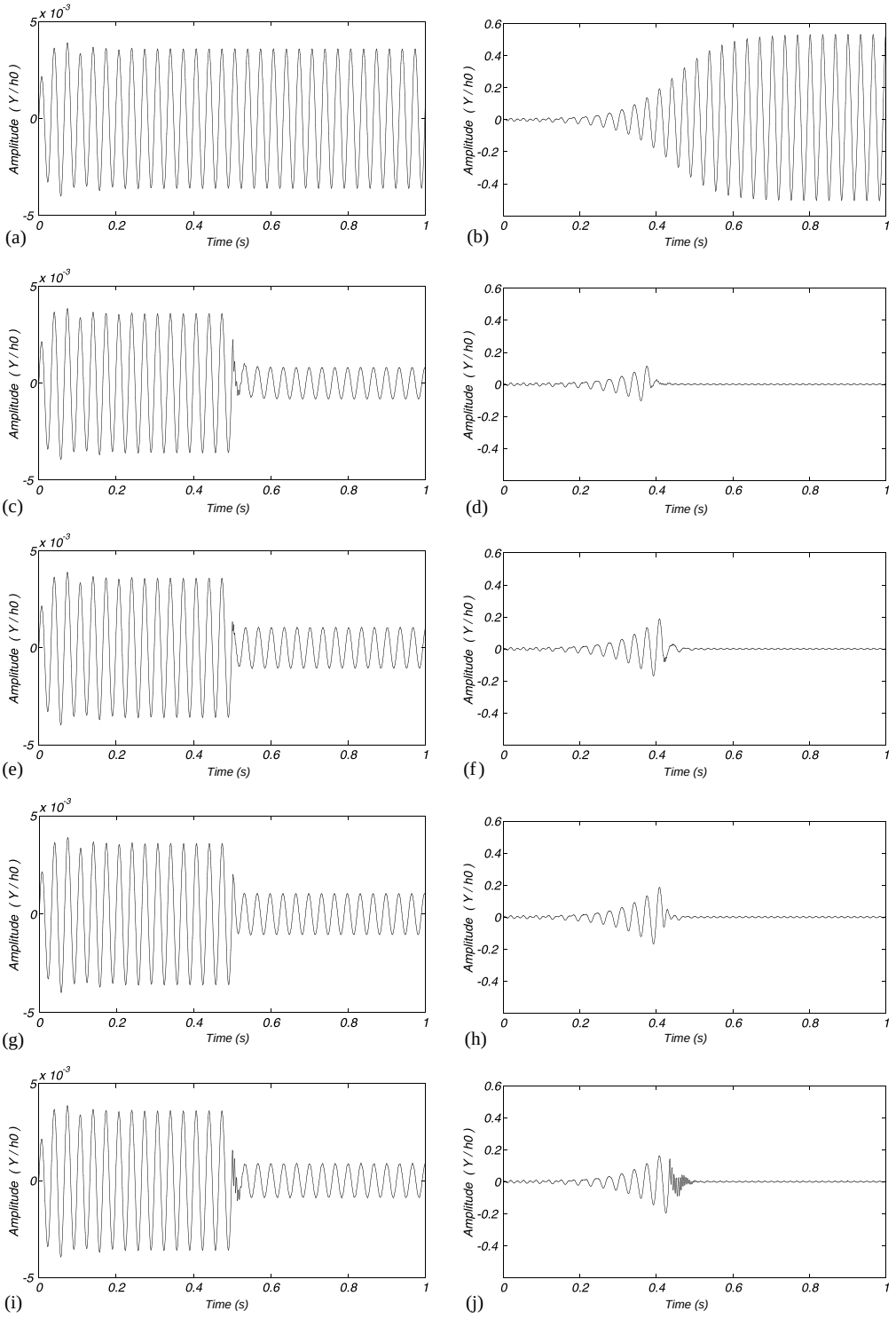

Fig. 14. Time response functions of the passive and active systems—control activated at $t = 0.5$ s or $Y/h_0 \geqslant \pm 0.2$: (a) $\dot{\phi} = 30$ Hz, passive; (b) $\dot{\phi} = 60$ Hz, passive; (c) $\dot{\phi} = 30$ Hz, PI; (d) $\dot{\phi} = 60$ Hz, PI; (e) $\dot{\phi} = 30$ Hz, PD; (f) $\dot{\phi} = 60$ Hz, PD; (g) $\dot{\phi} = 30$ Hz, PID; (h) $\dot{\phi} = 60$ Hz, PID; (i) $\dot{\phi} = 30$ Hz, non-linear P; (j) $\dot{\phi} = 60$ Hz, non-linear P.

by the active system. In addition, a decrease of vibration amplitude was achieved and the stability limit was shifted towards higher frequencies.

In the frequency response analysis, unsatisfactory results were obtained by using the proposed PI and PID controllers, specially in the loading direction (vertical). The most efficient controllers were those which did not eliminate the rotor eccentricity in the bearing. The fact of suppressing rotor eccentricity tends to decrease the oil film damping in the direction of this eccentricity. As a result, such a damping reduction has to be overcome and compensated by the controllers. The proposed PI and PID controllers were not able to achieve this task, resulting in higher responses than those of the passive system. However, it is important to note that the control laws with integral terms (PI and PID) may also lead to satisfactory results whenever the control system has enough power to supply to the system, in order to overcome the damping loss due to rotor centring.

For the design of controllers with integral part, it is of significant importance to analyse the K–D diagrams, like those present in Fig. 6, to assure that the integral part of the controller will not contribute to the reduction of the oil film damping. In the case of tilting-pad journal bearings, only the coefficients of the main diagonal of stiffness and damping matrices are of interest, since the cross-coupling coefficients are negligible. In the case of other actively lubricated journal bearings, this analysis becomes more complex, since the cross-coupling coefficients must not be disregarded.

Hence, the proposed non-linear P and the PD controllers were better suited to reduce vibration amplitudes of the rotor-bearing system, in the frequency range of study. Tests are being led in the rig illustrated in Fig. 3, in order to experimentally validate the theoretical results presented in this work.

Acknowledgements

The Brazilian research foundation FAPESP—Fundação de Amparo à Pesquisa do Estado de São Paulo—is greatfully acknowledged for the support given to this project.

References

[1] R. Stanway, C.R. Burrows, Active vibration control of a flexible rotor on flexibly-mounted journal bearings, American Society of Mechanical Engineers, Journal of Dynamic Systems, Measurement, and Control 103 (1981) 383–388.

[2] S. Fürst, H. Ulbrich, An active support system for rotors with oil-film bearings, IMechE, International Conference on Vibrations in Rotating Machinery, England, 1984, pp. 61–67.

[3] M.J. Goodwin, M.P. Roach, J.E.T. Penny, Variable impedance hydrodynamic journal bearings for controlling flexible rotor vibrations, 12th Biennial ASME Conference on Vibration and Noise, Montreal, Canada, 1989, pp. 261–267.

[4] I.F. Santos, Aktive Kippsegmentlagerung—theorie und experiment, Fortschritt-Berichte VDI Reihe 11, vol. 189, 1993.

[5] I.F. Santos, Design and evaluation of two types of active tilting-pad bearings, IUTAM Symposium on Active Control of Vibration, Bath, UK, 1994, pp. 79–87.

[6] H. Ulbrich, Active vibration control of rotors, Fifth ITToMM International Conference on Rotor Dynamics, Darmstadt, Germany, 1998, pp. 16–31.
[7] Y.K. Wang, C.D. Mote Jr., Active and passive vibration control of an axially moving beam by smart hybrid bearings, Journal of Sound and Vibration 195 (4) (1996) 575–584.
[8] W.X. Wu, F. Pfeiffer, Active vibration damping for rotors by a controllable oil-film bearing, Fifth IFToMM International Conference on Rotor Dynamics, Darmstadt, Germany, 1998, pp. 431–443.
[9] I.F. Santos, F.H. Russo, Tilting-pad journal bearings with electronical radial injection, American Society of Mechanical Engineers, Journal of Tribology 120 (3) (1998) 583–594.
[10] I.F. Santos, R. Nicoletti, THD analysis in tilting-pad journal bearings using multiple orifice hybrid lubrication, American Society of Mechanical Engineers, Journal of Tribology 121 (4) (1999) 892–900.
[11] I.F. Santos, R. Nicoletti, Influence of orifice distribution on the thermal and static properties of hybridly lubricated bearings, International Journal of Solids and Structures 38 (10–13) (2001) 2069–2081.
[12] I.F. Santos, A. Scalabrin, Control system design for active lubrication with theoretical and experimental examples, ASME/IGTI International Gas Turbine and Aeroengine Congress and Exhibition, Munich, Germany, 2000-GT-643, 2000.
[13] D.E. Bently, J.W. Grant, P. Hanifan, Active controlled hydrostatic bearing for a new generation of machines, ASME/IGTI International Gas Turbine and Aeroengine Congress and Exhibition, Munich, Germany 2000-GT-354, 2000.
[14] I.F. Santos, A. Scalabrin, R. Nicoletti, Ein Beitrag zur aktiven Schmierungstheorie, in: H. Irretier, R. Nordmann, H. Springer (Eds.), Schwingungen in rotierenden Machinen V, Vol. 5, Vieweg Verlag, Berlin, 2001, pp. 21–30.
[15] R. Nicoletti, I.F. Santos, Vibration control of rotating machinery using active tilting-pad bearings, IEEE/ASME International Conference on Advanced Mechatronics, Como, Italy, 2001.
[16] W.J. Thayer, Transfer functions for MOOG servovalves, MOOG Technical Bulletin, Vol. 103, 1965.
[17] M. Rashidi, E. Dirusso, Design of a hydraulic actuator for active control of rotating machinery, American Society of Mechanical Engineers, Journal of Engineering for Gas Turbines and Power 115 (1993) 336–340.
[18] W.R. Evans, Control system synthesis by root locus method, AIEE Transactions—Part II 69 (1950) 66–69.
[19] K. Ogata, Discrete-time control systems, Prentice-Hall, Upper Saddle River, NJ, 1995.
[20] H. Springer, Dynamische Eigenshaften von Gleitlagern mit beweglischen Segmenten, VDI-Berichte 381 (1980) 177–184.
[21] A. Muszynska, Stability of whirl and whip in rotor/bearing systems, Journal of Sound and Vibration 127 (1) (1988) 49–64.
[22] R.D. Flack, C.J. Zuck, Experiments on the stability of two flexible rotors in tilting pad bearings, STLE Tribology Transactions 31 (2) (1988) 251–257.
[23] Y. Lie, X. You-Bai, Z. Jun, Q. Damou, Experiments on the destabilizing factors in tilting-pad bearings, Tribology International 22 (5) (329–334).
[24] M.F. White, S.H. Chan, The subsynchrounous dynamic behaviour of tilting-pad journal bearings, American Society of Mechanical Engineers, Journal of Tribology 114 (1) (1992) 167–173.
[25] K.O. Olsson, Some fundamental aspects on the dynamic properties of journal bearings, Sixth International Conference on Vibrations in Rotating Machinery, IMechE, London, UK, 1986, pp. 31–40.